数理解析研究所講究録
1142 巻 2000 年 36-52

Implementation of the Collins-Kim-Holton Algorithm to Solve the Deutsch's Problem on One-, Two-, and Three-Qubit NMR Quantum Computers

Ushio Sakaguchi,[a] Hiroshi Ozawa,[b] Chikara Amano,[c]
Toshio Fukumi,[d] William S. Price[e]
(坂口 潮, 小澤 宏, 天野 力, 福見俊夫, William S. Price)

[a]*Kumamoto Gakuen University, Kumamoto 862-8680, Japan*
[b]*Information Technology Center, The University of Tokyo, Tokyo 113-8658, Japan*
[c]*Department of Chemistry, Kanagawa University, Hiratsuka 259-1293, Japan*
[d]*Osaka National Research Institute, Ikeda 563-8577, Japan*
[e]*Water Research Institute, Tsukuba 305-0047, Japan*

Abstract

The Collins-Kim-Holton algorithm to solve the Deutsch's problem is implemented for the first time on one-, two-, and three-qubit nuclear magnetic resonance (NMR) quantum computers. The one-qubit case is the simplest example of implementation of any nontrivial quantum algorithm. The three-qubit case is the first meaningful test of quantum algorithms to solve the Deutsch's problem in that entangled states are involved. In the three-qubit case, a new approach which uses a field gradient pulse immediately before signal acquisition is adopted to implement the algorithm which is otherwise almost impossible to perform by NMR.

1 Introduction

Quantum computation is an exciting and rapidly growing field of research [1–6]. Most previous studies centered on theoretical aspects, mainly because the practical realization of quantum computers is difficult. A quantum computer uses a quantum system to store information, manipulates the system states through unitary transformations, and extract useful information from the resulting state. To this end, a quantum system should be protected from the

effect of decoherence, which might destroy the information stored in the quantum system. Decoherence is now considered to be the biggest obstacle to realizing any quantum computer.

Recently several groups proposed the use of nuclear magnetic resonance (NMR) quantum computers and demonstrated their usefulness [7–27]. Nuclear spin systems are rather well isolated from the environment and have longer decoherence times. The first quantum algorithm that was implemented on any quantum computer was the Deutsch-Jozsa algorithm to solve the Deutsch's problem [28] (see below) and these implementations employed NMR [15–17]. The algorithm for the two-qubit (quantum bit) case has been implemented by Chuang *et al.* [15] and Jones and Mosca [16] and more recently implementation of the three-qubit case has been reported by Linden, Barjat, and Freeman [17]. The Deutsch-Jozsa algorithm has been refined recently by Collins, Kim, and Holton (CKH) [18]. The CKH algorithm allows the size of a quantum computer to be reduced by one qubit than the original algorithm. Thus, previous implementations correspond to cases of one- and two-qubits in this modified algorithm.

We here report the results of implementation of the CKH algorithm to solve the Deutsch's problem on one-, two-, and three-qubit NMR quantum computers. The one-qubit case is, of course, the simplest example of implementation of any nontrivial quantum algorithm and shows that even a quantum computer with only one qubit can be used to solve a problem. The three-qubit case constitutes the first meaningful test of the CKH algorithm. As CKH pointed out [18], any meaningful test of their algorithm (and the Deutsch-Jozsa algorithm) occurs if and only if the number of qubits of a quantum computer is greater than two. The three-qubit case involves entangled states whereas previous implementations cited above did not exploit entangled states which are considered to be responsible for the power of quantum computers.

The Deutsch's problem [28] may be stated as follows: "Given an unknown function $f(x)$ that maps N bits to one bit. Determine whether the function is constant or balanced using only one function call (function evaluation)." Here "balanced" means that the function gives an equal number of 0 and 1 outputs.

On a classical deterministic computer, at least $2^{N-1}+1$ function calls are required to tell with certainty that the function is really constant or not. For example, in the simplest one-bit case where $f(x)$ is a function on only one bit, we need to evaluate both $f(0)$ and $f(1)$ to determine whether it is balanced or constant. Namely, two function calls are necessary classically. In quantum algorithms (the Deutsch-Jozsa and the CKH algorithms), only one function call suffices (see below).

The CKH algorithm which was implemented in this study works as follows.

Suppose that a quantum computer is made of N qubits and prepared in the state $|0\rangle|0\rangle\cdots|0\rangle$, where $|0\rangle$ (or $|1\rangle$) refers to the spin up (or down) state of a nuclear spin in an external magnetic field. First we apply the Hadamard transformation H which is defined by

$$H = \frac{1}{\sqrt{2}}\begin{pmatrix} 1 & 1 \\ 1 & -1 \end{pmatrix} \tag{1}$$

upon each qubit, producing an equally weighted superposition

$$(|0\rangle + |1\rangle)(|0\rangle + |1\rangle)\cdots(|0\rangle + |1\rangle) = \sum_{x=0}^{2^N-1} |x\rangle \,, \tag{2}$$

where x stands for a binary number $x = x_1x_2\cdots x_N$. Also here and henceforth we omit normalization constants. The unitary transformation U_f that performs function evaluation is defined in the CKH algorithm by

$$U_f : \quad |x\rangle \to (-1)^{f(x)}|x\rangle \,. \tag{3}$$

In the original Deutsch-Jozsa algorithm, function evaluation was defined by the transformation

$$U_f : \quad |x\rangle|y\rangle \to |x\rangle|y \oplus f(x)\rangle \,, \tag{4}$$

and at least two qubits were necessary for any implementation. We then apply U_f defined in Eq. (3) to the above state in superposition, yielding the state

$$\sum_x (-1)^{f(x)}|x\rangle \,. \tag{5}$$

Finally we apply the Hadamard transformation H again to obtain the final state

$$\sum_x \sum_y (-1)^{f(x)}(-1)^{x*y}|y\rangle \,, \tag{6}$$

where $x * y$ is the sum $(mod\ 2)$ of the bitwise product of $x = x_1x_2\cdots x_N$ and $y = y_1y_2\cdots y_N$:

$$x * y = x_1y_1 \oplus x_2y_2 \oplus \cdots \oplus x_Ny_N \,. \tag{7}$$

Now, if $f(x)$ is constant,

$$\begin{aligned}\sum_x \sum_y (-1)^{f(x)}(-1)^{x*y}|y\rangle &= (-1)^{f(0)} \sum_y (\sum_x (-1)^{x*y})|y\rangle \\ &= (-1)^{f(0)} \sum_y \delta_{y0}|y\rangle \\ &= (-1)^{f(0)}|0\rangle \ , \end{aligned} \tag{8}$$

while if $f(x)$ is balanced, the amplitude of the state $|0\rangle$ is given by

$$\sum_x (-1)^{f(x)} = 0 \ , \tag{9}$$

because $f(x)$ contains an equal number of 0s and 1s. Thus, after the series of operations $H \rightarrow U_f \rightarrow H$, the amplitude of the state $|0\rangle|0\rangle \cdots |0\rangle$ in the final state of the quantum computer tells with certainty whether the function is constant or balanced. Note in the above we made the function call only once. Note also that the last amplitude measurement can not be implemented directly on NMR, except in the simplest one-qubit case.

2 The One- and Two-Qubit Cases *vs.* the Three-Qubit Case

In the one-qubit case, the algorithm becomes quite simple. Starting from the state $|0\rangle$, we apply H to yield the state $|0\rangle + |1\rangle$. There are four functions that map one bit to one bit. Constant functions are $f_{00}(x) = 0$ and $f_{11}(x) = 1$ for both $x = 0$ and 1. Balanced functions are $f_{01}(x) = x$ and $f_{10}(x) = 1 - x$. Upon application of $U_{f_{00}}$ (or $U_{f_{11}}$) on the state $|0\rangle + |1\rangle$, we get the state $|0\rangle + |1\rangle$ (or $-(|0\rangle + |1\rangle)$). The second Hadamard transformation of this state gives rise to the state $|0\rangle$ (or $-|0\rangle$) as the final state. On the other hand, application of the balanced function f_{01} (or f_{10}) generates the state $|0\rangle - |1\rangle$ (or $-(|0\rangle - |1\rangle)$, which, after the second Hadamard transformation, becomes the state $|1\rangle$ (or $-|1\rangle$). Thus, if we look at the final state, we can tell with certainty whether the function is constant or balanced.

In the two qubit case, the state $(|0\rangle + |1\rangle)(|0\rangle + |1\rangle)$ obtained by applying the first Hadamard transformation H on the starting state $|0\rangle|0\rangle$ is transformed by one of the eight U_fs, yielding the states

$$\pm(|0\rangle + |1\rangle)(|0\rangle + |1\rangle) \tag{10}$$

for constant functions and

$$\pm(|0\rangle - |1\rangle)(|0\rangle + |1\rangle) \quad \text{or}$$
$$\pm(|0\rangle - |1\rangle)(|0\rangle - |1\rangle) \quad \text{or}$$
$$\pm(|0\rangle + |1\rangle)(|0\rangle - |1\rangle) \tag{11}$$

for six balanced functions. The final states are

$$\begin{aligned}
&\pm|0\rangle|0\rangle \quad \text{for} \quad f_{0000} \quad \text{and} \quad f_{1111}\,, \\
&\pm|1\rangle|0\rangle \quad \text{for} \quad f_{0011} \quad \text{and} \quad f_{1100}\,, \\
&\pm|1\rangle|1\rangle \quad \text{for} \quad f_{0110} \quad \text{and} \quad f_{1001}\,, \quad \text{and} \\
&\pm|0\rangle|1\rangle \quad \text{for} \quad f_{0101} \quad \text{and} \quad f_{1010}\,.
\end{aligned} \tag{12}$$

We can discriminate not only constant from balanced functions but also these four groups. For example, if we apply a hard (non-selective) $\pi/2$ read-pulse, and if we denote the first and second spins as I and S, respectively, the resulting spectrum of the two (I and S) doublets should appear both upward for constant functions but down-up or down-down or up-down doublets for balanced functions. Alternatively, we may apply a soft (selective) $\pi/2$ read-pulse only to the spin I, for example, in which case only one peak of the I doublet will appear upward and at a position corresponding to the partner spin S being in the state $S_z = \alpha$ ($|0\rangle$) for constant functions. For balanced functions $U_{f_{0011}}$ and $U_{f_{1100}}$, a downward singlet will be seen at the same position while the other balanced functions will give rise to a single peak at a position corresponding to $S_z = \beta$ ($|1\rangle$). Alternatively again, we may use a selective $(\pi/2)_x(S)$ pulse, where the pulse notation refers to a $\pi/2$ pulse along the x-axis (of the rotating frame of reference) on spin S. These three methods of detection serve to a complete characterization of the final states and we performed all the three.

In both of the one- and two-qubit cases, no entangled state appears anywhere. This makes a sharp contrast to the three-qubit case. In the three-qubit case, there are 70 balanced functions, of which half can be seen to give the same spectra as the remaining half. These 35 balanced functions and their corresponding U_f operators are summarized in Table 1.

Final states are in general entangled. For example, the balanced function $f_{00010111}$, which belongs to group I, gives the state $(|01\rangle + |10\rangle)|0\rangle + (|00\rangle - |11\rangle)|1\rangle$ as the final state:

$$\begin{aligned}
|0\rangle|0\rangle|0\rangle \quad &\xrightarrow{H} \quad \sum_x |x\rangle \\
&\xrightarrow{U_f} \quad (|00\rangle - |11\rangle)(|0\rangle + |1\rangle) + (|01\rangle + |10\rangle)(|0\rangle - |1\rangle) \\
&\xrightarrow{H} \quad (|01\rangle + |10\rangle)|0\rangle + (|00\rangle - |11\rangle)|1\rangle\,.
\end{aligned} \tag{13}$$

In general it may be difficult, if not impossible, to examine the amplitude of

Table 1
Balanced functions in the three-qubit case, grouped into nine categories.

group	representative function	U_f operator	total number*
A	$f_{00001111}$	$e^{i\pi I_z}$	3
B	$f_{00111100}$	$e^{i\pi I_z}e^{i\pi S_z}$	3
C	$f_{01101001}$	$e^{i\pi(I_z+S_z+K_z)}$	1
D	$f_{00101101}$	$e^{i\pi I_z}e^{i\frac{\pi}{2}(S_z-K_z)}e^{i\pi S_zK_z}$	3
	$f_{01001011}$	$e^{i\pi I_z}e^{i\frac{\pi}{2}(S_z-K_z)}e^{-i\pi S_zK_z}$	3
E	$f_{00011110}$	$e^{i\pi I_z}e^{i\frac{\pi}{2}(S_z+K_z)}e^{i\pi S_zK_z}$	3
	$f_{10000111}$	$e^{i\pi I_z}e^{i\frac{\pi}{2}(S_z+K_z)}e^{-i\pi S_zK_z}$	3
F	$f_{00011011}$	$e^{i\frac{\pi}{2}(I_z+S_z)}e^{i\pi K_zI_z}e^{-i\pi K_zS_z}$	3
	$f_{00100111}$	$e^{i\frac{\pi}{2}(I_z+S_z)}e^{-i\pi K_zI_z}e^{i\pi K_zS_z}$	3
G	$f_{01001110}$	$e^{i\frac{\pi}{2}(I_z-S_z)}e^{i\pi K_zI_z}e^{i\pi K_zS_z}$	3
	$f_{10001101}$	$e^{i\frac{\pi}{2}(I_z-S_z)}e^{-i\pi K_zI_z}e^{-i\pi K_zS_z}$	3
H	$f_{10001110}$	$e^{i\frac{\pi}{2}(I_z-S_z-K_z)}e^{-i2\pi I_zS_zK_z}$	3
I	$f_{00010111}$	$e^{i\frac{\pi}{2}(I_z+S_z+K_z)}e^{-i2\pi I_zS_zK_z}$	1

* Operators which will be obtained by cyclically permuting I_z, S_z, and K_z are not shown in the table. Only the total numbers are listed.

the state $|0\rangle|0\rangle\cdots|0\rangle$ in such final states (in superposition of states) and to obtain a clear-cut analysis by NMR, because NMR performs a deterministic measurement on a Avogadro's number of identical molecules.

However, we note here that the transverse relaxation causes the loss of the phase coherence of the transverse magnetization. The transverse relaxation time (T_2) is shorter than or equal to the longitudinal relaxation time (T_1) and it is well known that usually the T_2 process is much faster than the T_1 process [29]. This means that if we allow such a final spin state to decohere for a time of order T_2, only the diagonal part of the density matrix remains (If we allow the spins to decohere for much longer times, the spin system will attain the thermal equilibrium state and any remaining information will be lost due to the longitudinal relaxation). For example, the density operator after T_2 decoherence of the above entangled state is given, in the product operator formalism [29], by

$$\rho = (1 - 8I_zS_zK_z)/2\,, \tag{14}$$

where I refers to the first spin, S to the second, and K to the third, and we omitted proportionality constants. Equation (14) holds for U_fs of group H, as well as group I. We can see that the other balanced functions should yield similarly

$$\begin{aligned}
&\rho = (1-2I_z)(1+2S_z)(1+2K_z)/8 \quad \text{for group A}\,,\\
&\rho = (1-2I_z)(1-2S_z)(1+2K_z)/8 \quad \text{for group B}\,,\\
&\rho = (1-2I_z)(1-2S_z)(1-2K_z)/8 \quad \text{for group C}\,,\\
&\rho = (1-2I_z)/2 \quad \text{for groups D and E}\,,\\
&\rho = (1-4I_zS_z)/2 \quad \text{for groups F and G}\,,\\
&\qquad \text{and their cyclic permutations of } I_z,\ S_z, \text{ and } K_z\\
&\qquad \text{except for group C}\,,
\end{aligned} \tag{15}$$

while constant functions should give

$$\rho = (1+2I_z)(1+2S_z)(1+2K_z)/2\,. \tag{16}$$

These states are far simpler than otherwise and allow an easy and straightforward distinction to be made between constant and balanced functions.

Note further that the same effect can be obtained experimentally by application of the pulsed field gradient along the z-axis (G_z), which is known [29] to annihilate only the transverse magnetization while preserving the longitudinal one, hence the name "purging pulse" or "purging gradient." The state $|000\rangle$ which results as the final state for constant functions is unaffected by the transverse decoherence (T_2 relaxation) nor by G_z. Thus, we may solve the Deutsch's problem in the three-qubit case also by NMR if we insert this procedure immediately before measurement. We employed this procedure for the three-qubit case. It is easy to see that this method can be used to spin systems containing more spins, because constant functions always regenerate, as the final state after decoherence, the starting state $|0\cdots0\rangle$, but balanced functions should yield density operators definitely different from $|0\cdots0\rangle\langle0\cdots0|$ (containing no contribution from $|0\cdots0\rangle\langle0\cdots0|$).

3 Thermal State as an Input

In the above, the states $|0\rangle$ and $|1\rangle$ represent either pure states or effective pure states. However, we note that to solve the Deutsch's problem only, we do not need to prepare (effective) pure states and thermal states suffices. This is because, as we will show below, we can discriminate constant from balanced functions even if we started from thermal states. This is not the first time it

was realized that thermal input states are sufficient to implement a quantum algorithm [17,24]. Therefore, we started from the thermal state in one- and three-qubit cases.

Only in the two-qubit case, we prepared actually the effective pure state $|0\rangle|0\rangle$ as an input from thermal state by the method of spatial labelling, in order to show that a variety of methods for signal detection can be used to attain our goal (see above).

Let us examine briefly the behaviour of the density operator when we start from thermal state. In the one-qubit case, the density operator describing the state of an ensemble of one-spin molecules at thermal equilibrium in an external magnetic field can be written, if we omit proportionality constants, as

$$\rho_{eq} = I_z \ . \tag{17}$$

It is easy to see that this starting state is eventually transformed into $\rho = I_z$ for constant functions and $\rho = -I_z$ for balanced functions. An NMR peak after applying the $\pi/2$ read-pulse will appear upward for the former but downward for the latter.

In the three qubit case, if we use thermal state as an input, the density operator of this starting state is written in the same way as before as

$$\rho_{eq} = I_z + S_z + K_z \ . \tag{18}$$

After application of the sequence $H \rightarrow U_f \rightarrow H \rightarrow G_z$, constant functions regenerates the same state, $\rho = I_z + S_z + K_z$, because of H being self-inverse ($HH = 1$), while balanced functions yield

$$\begin{aligned}
&\rho = -I_z + S_z + K_z \quad \text{for group A ,} \\
&\rho = -I_z - S_z + K_z \quad \text{for group B ,} \\
&\rho = -I_z - S_z - K_z \quad \text{for group C ,} \\
&\rho = -I_z \qquad\qquad\ \ \text{for groups D and E ,} \\
&\rho = 0 \qquad\qquad\ \ \text{for groups F, G, H, and I ,} \\
&\qquad \text{and their cyclic permutations of } I_z, S_z, \text{ and } K_z \\
&\qquad \text{for groups A, B, D, and E .}
\end{aligned} \tag{19}$$

For example, in the case of $f_{10001110}$, which belongs to group H, the density operator is transformed as

$$\rho_{eq} = I_z + S_z + K_z \quad \xrightarrow{H} \quad \rho = I_x + S_x + K_x$$

$$\begin{aligned} &\xrightarrow{U_f} && \rho = 4I_xS_zK_z - 4I_zS_xK_z - 4I_zS_zK_x \\ &\xrightarrow{H} && \rho = 4I_zS_xK_x - 4I_xS_zK_x - 4I_xS_xK_z \\ &\xrightarrow{G_z} && \rho = 0 \ , \end{aligned} \tag{20}$$

which is easily seen if we use the relation

$$e^{-i2\pi I_zS_zK_z} I_x e^{i2\pi I_zS_zK_z} = 4I_yS_zK_z \ . \tag{21}$$

If we apply a hard $\pi/2$ read-pulse, constant functions will yield all three (I, S, and K) quartets pointing upward, whereas balanced functions will exhibit three quartets pointing downward somewhere (groups A, B, and C), or either only one (I) quartet appearing downward (groups D and E), or no quartet at all (groups F, G, H and I). Thus, we can determine whether the function is constant or balanced in a single experiment.

4 Implementation

The first step of the CKH algorithm starts with the Hadamard transformation H, which corresponds to the operator $e^{-i\frac{\pi}{2}} e^{i\pi I_x} e^{-i\frac{\pi}{2}I_y}$ and was simply implemented by a $(-\pi/2)_y$ pulse. The transformation H that is used in the last step of the algorithm was executed by a $(\pi/2)_y$ pulse in order to assure that H is self-inverse.

In the one-qubit case, transformations $U_{f_{00}}$ and $U_{f_{11}}$ were simply "doing nothing." Transformations $U_{f_{10}}$ and $U_{f_{01}}$ correspond to the operator $e^{i\pi I_z}$ apart from an irrelevant overall phase-factor and were implemented by the pulse sequence $(\pi)_x - (\pi)_y$, where the pulse sequence should be read from left to right as " a $(\pi)_x$ pulse followed by a $(\pi)_y$ pulse."

In the two-qubit case, there are six balanced and two constant functions. For these the U_f transformations are implemented as given in Table 2. All the operators for balanced functions are of the form $e^{-i\pi I_z}$ or $e^{i\pi S_z}$ or $e^{-i2\pi I_zS_z}$.

As seen from Tables 1 and 2, the unitary transformation (U_fs) in one-, two-, and three-qubit cases all consist of terms of the form $e^{\pm i\frac{\pi}{2}I_z}$, $e^{\pm i\pi I_z}$, $e^{\pm i\pi I_zS_z}$, $e^{\pm i2\pi I_zS_z}$, and $e^{\pm i2\pi I_zS_zK_z}$, and their cyclic permutations of I_z, S_z, and K_z. The terms $e^{\pm i\frac{\pi}{2}I_z}$ and $e^{\pm i\pi I_z}$ were implemented by the pulse sequences $(-\frac{\pi}{2})_y(I) - (\pm\frac{\pi}{2})_x(I) - (\frac{\pi}{2})_y(I)$ and $(\pm\pi)_x(I) - (\pi)_y(I)$, respectively. The unitary operators $e^{i\pi I_zS_z}$ and $e^{i2\pi I_zS_z}$ were implemented as the sequence $\tau - (\pi)_x(I), (\pi)_x(S) - \tau - (\pi)_x(I), (\pi)_x(S)$ where τ is the free precession period of length $\tau = 1/4J_{IS}$ and $\tau = 1/2J_{IS}$, respectively. If we note the relation

Table 2
The unitary operators (U_fs) in the two-qubit case.

U_f		operator	pulse sequence*
U_{f0000}	U_{f1111}	1	doing nothing
U_{f0011}	U_{f1100}	$e^{-i\pi I_z}$	$(-\pi)_x(I) - (\pi)_y(I)$
U_{f0110}	U_{f1001}	$e^{-i2\pi I_z S_z}$	$\tau - (\pi)_x(I), (\pi)_x(S) - \tau - (\pi)_x(I), (\pi)_x(S)$
U_{f0101}	U_{f1010}	$e^{i\pi S_z}$	$(\pi)_x(S) - (\pi)_y(S)$

* $\tau = 1/2J_{IS}$

$$e^{-i2\pi I_z S_z K_z} = e^{-i\frac{\pi}{2}I_x} e^{-i\pi I_z K_z} e^{-i\frac{\pi}{2}I_y} e^{-i\pi I_z S_z} e^{i\frac{\pi}{2}I_y} e^{i\pi I_z K_z} e^{i\frac{\pi}{2}I_x}, \tag{22}$$

the operator $e^{\pm i2\pi I_z S_z K_z}$ will be seen to be implemented by a proper combination of the above pulse sequences.

5 Experimental

All the experiments were done on a Bruker DMX 500 spectrometer (^{1}H operating frequency 500 MHz) at room temperature (about 298 K). As the water sample for the one-spin case we used actually D_2O (Showa Denko, nominal purity > 99 %) as supplied to avoid the radiation damping. The residual water signal gave a strong enough signal. For the two-spin experiment, we employed *trans*-cinnamic acid (C_6H_5-CH=CH(COOH)) dissolved in $CDCl_3$ ($\sim$ 0.65 M/l), whose olefinic protons have a chemical shift of 671 Hz and a spin-spin coupling constant J =16.0 Hz. The selective pulses were Gaussian in form and centered on each doublet. We did not use any window function prior to Fourier transformation of the free induction decay.

6 Results and Discussion

Figure 1 shows the results of the one-qubit experiment. While a constant function yields an upward peak, a downward peak is obtained for a balanced function, as expected. This experiment corresponds, in essence, to the two-qubit implementations of the Deutsch-Jozsa algorithm made by Chuang *et al.* [15] and Jones and Mosca [16], but the present result demonstrates clearly

that even only one qubit can work as a quantum computer and can actually solve a problem.

Figures 2 to 4 give the results of the two-qubit experiment. In the two-qubit case, we started by preparing the effective pure state $|00\rangle$ and the final states given in Eq. (12) allow a variety of measurements. One can read out the final states by applying a non-selective $\pi/2$ pulse and Fourier transforming the resulting free induction decay. This result is given in Fig. 2.

Alternatively, one may use a selective $\pi/2$ read-pulse on spin I (or S), yielding the results of Fig. 3 (or Fig. 4). In order to completely characterize the final states, all these three are necessary. The three results are compared to the prediction (stick diagrams) in Figs. 2 to 4. In these figures, the agreement between the observed and the expected signals seems rather good, confirming basically that the CKH algorithm works properly in the first place and that our implementation is correct.

In Fig. 2, small anomalies are noted in the relative intensities in each doublet. Also, in Figs. 3 and 4, residual peaks are noted which, in theory, should not appear at all. These imperfections, for which we did not ascertain the origins, seem to arise from imperfect selectivity of "selective pulses" or from the decoherence (In the cases of Figs. 3 and 4, a total of five selective pulses are needed, apart from hard pulses and field-gradient pulses). The results of the three-qubit experiment will be reported elsewhere.

In conclusion, the present experiment demonstrates, for the first time, that (i) the CKH algorithm is valid for solving the Deutsch-Jozsa's problem, (ii) even one qubit can work as a quantum computer and solve an actual problem, and (iii) the CKH algorithm in the three-qubit case which involves entangled states can be implemented by NMR.

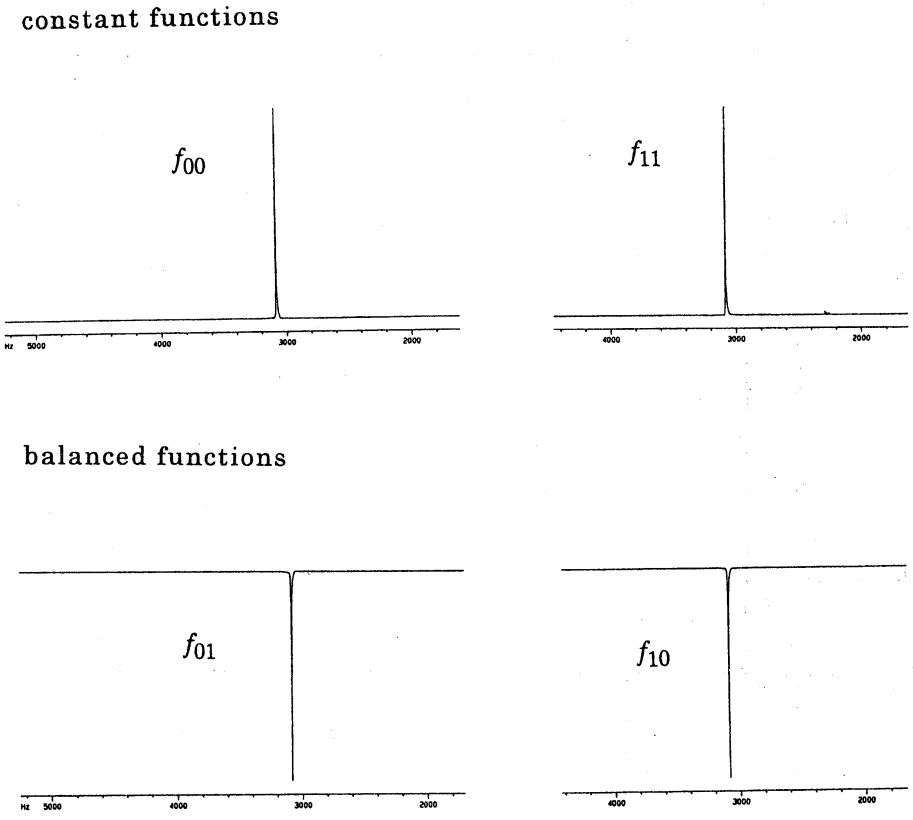

Fig. 1. The results of one-qubit NMR computation,"water experiment."

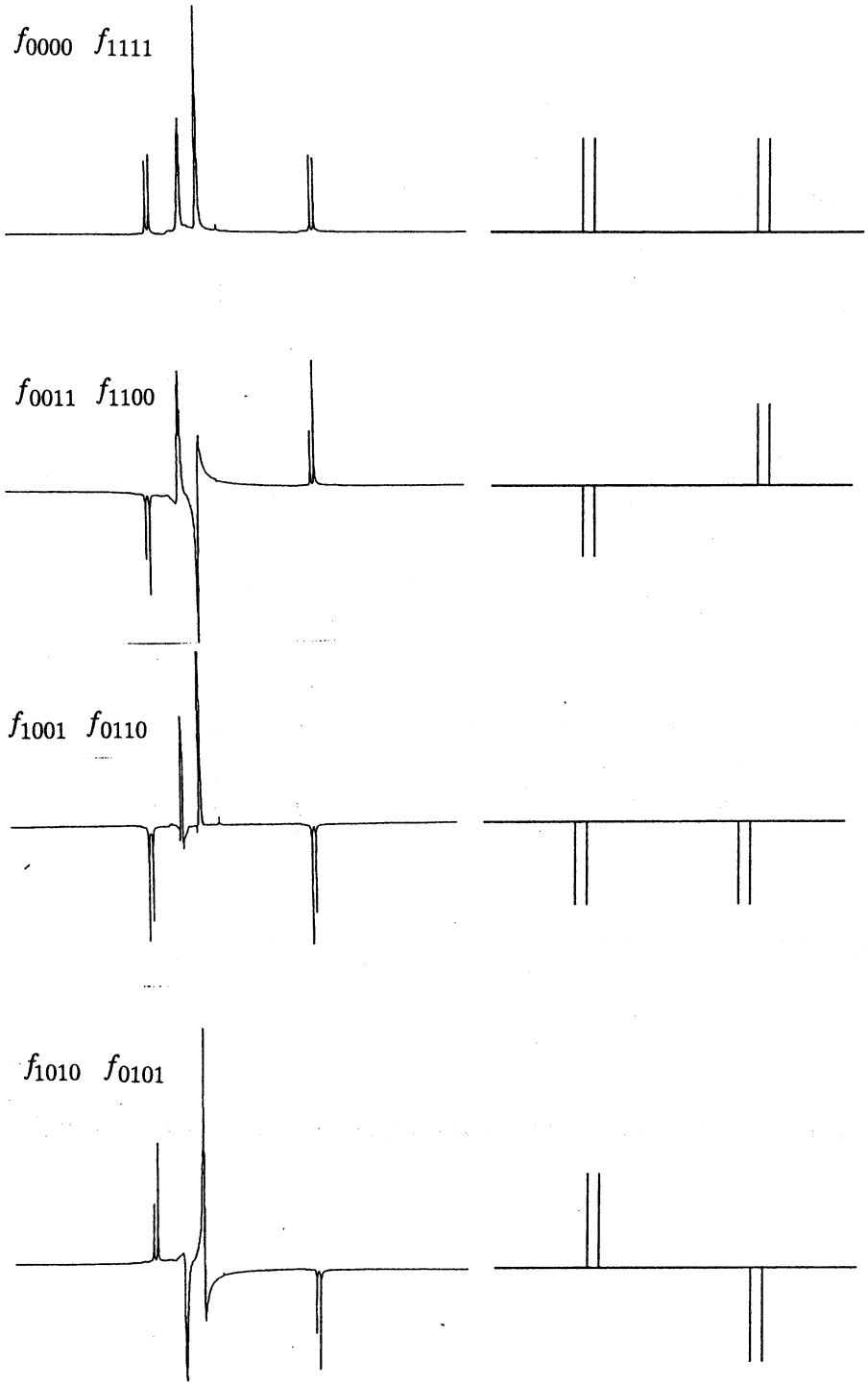

Fig. 2. The results of the two-qubit experiment. The computer molecule is *trans*-cinnamic acid dissolved in chloroform-*d*. Final states are read out by applying a non-selective $\pi/2$ pulse on both spins. The relevant peaks are the two outermost doublets. Ignore the two central peaks which are due to the phenyl group of the computer molecule and the residual solvent. The predicted spectra are given to the right as stick diagrams.

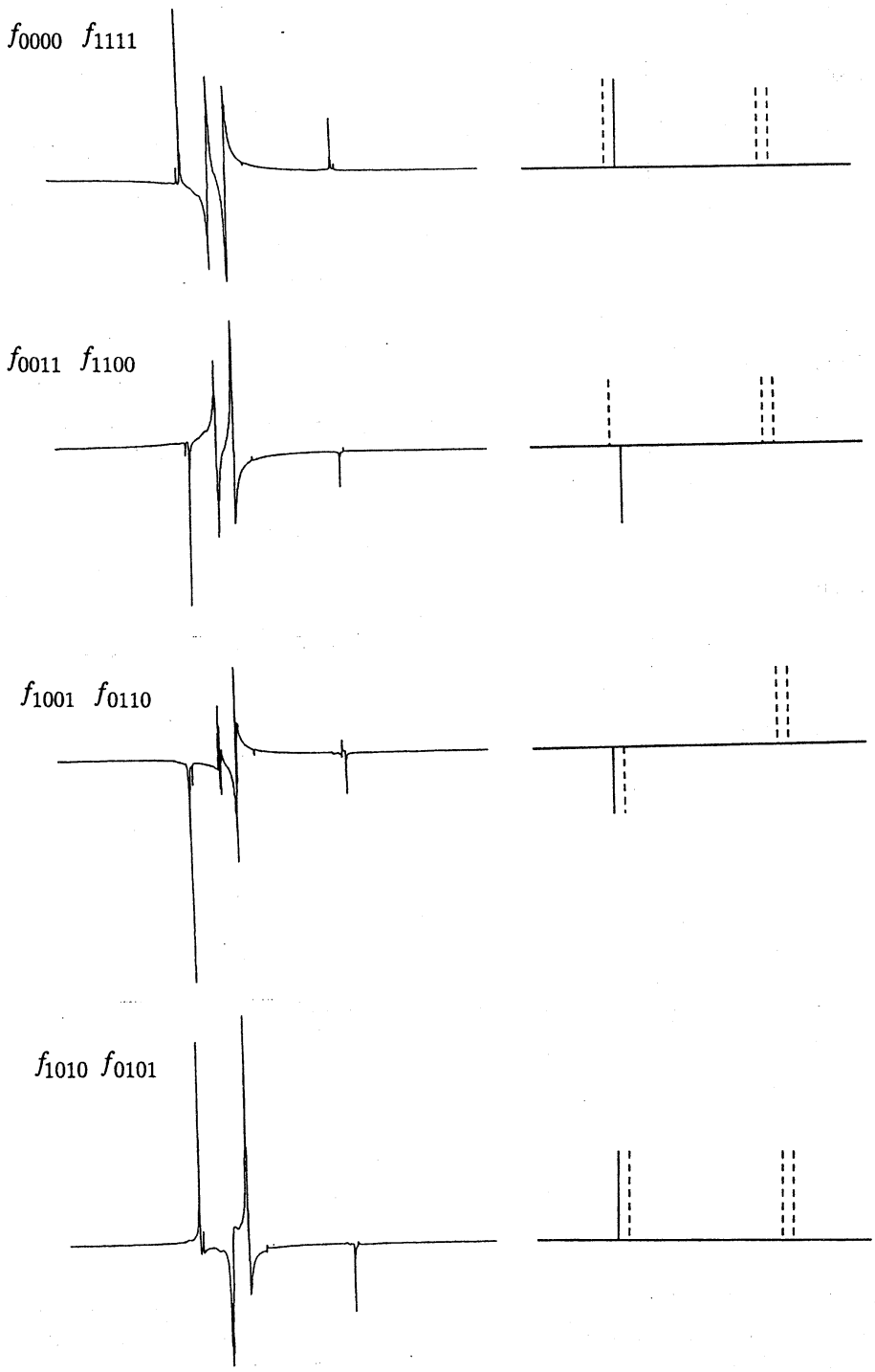

Fig. 3. The results of the two-qubit experiment, obtained by applying a selective $\pi/2$ read-pulse on spin I, which is to the left of the spectra. In the stick diagram, the dotted lines indicate peaks that are expected, in theory, to disappear. Other remarks are the same as in Fig. 2.

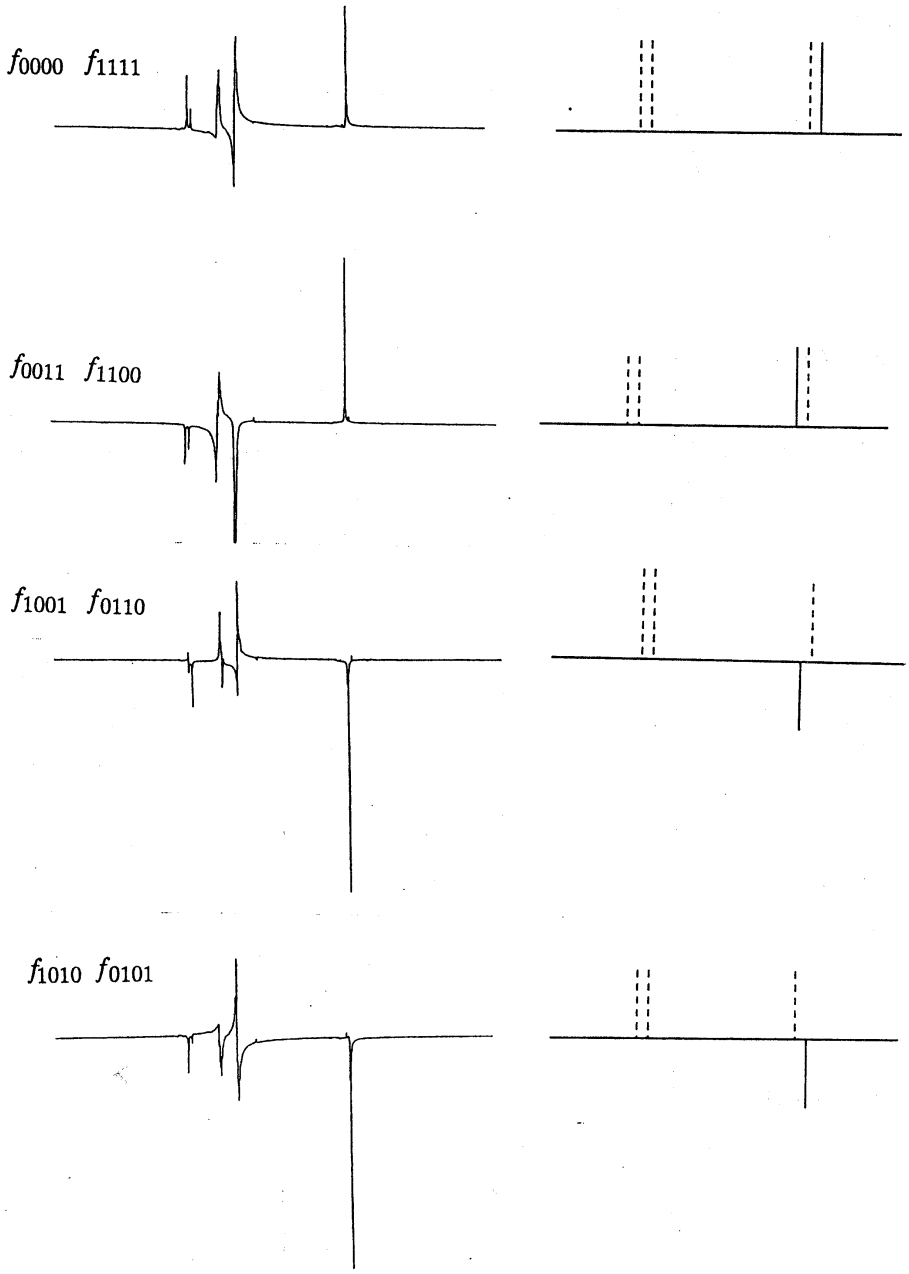

Fig. 4. The results of the two-qubit experiment, obtained by applying a selective $\pi/2$ read-pulse on spin S, which is to the right of the spectra. Other remarks are the same as in Figs. 2 and 3.

References

[1] A. Steane, "Quantum computing," Rept. Prog. Phys. **61**, 117-173 (1998).

[2] E. G. Rieffel and W. Polak, "An introduction to quantum computing for non-physicists," LANL e-print quant-ph/9809016.

[3] D. Aharonov, "Quantum computation," LANL e-print quant-ph/9812037; to appear in D. Stauffer, ed., *Annual Reviews of Computational Physics*, VI (World Scientific, 1998).

[4] V. Vedral and M. B. Plenio, "Basics of quantum computation," LANL e-print quant-ph/9802065; Prog. Quant. Electron. **22**, 1-40 (1998).

[5] R. Jozsa, "Entanglement and quantum computation," in S. Huggett, *et al.* eds., *Geometric Issues in the Foundations of Science* (Oxford University Press, 1997).

[6] D. P. DiVincenzo, "Quantum computation," Science **270**, 255-261 (1995).

[7] D. G. Cory, M. D. Price, and T. F. Havel, "Nuclear magnetic resonance spectroscopy: An experimentally accessible paradigm for quantum computing," Physica D **120**, 82-101 (1998).

[8] D. G. Cory, A. F. Fahmy, and T. F. Havel, "Ensemble quantum computing by NMR spectroscopy," Proc. Natl. Acad. Sci. USA **94**, 1634-1639 (1997).

[9] E. Knill, I. Chuang, and R. Laflamme, "Effective pure states for bulk quantum computation," Phys. Rev. A **57**, 3348-3363 (1998).

[10] N. A. Gershenfeld and I. L. Chuang, "Bulk spin resonance quantum computation," Science **275**, 350-356 (1997).

[11] I. L. Chuang, N. Gershenfeld, M. G. Kubinec, and D. W. Leung, "Bulk quantum computation with nuclear magnetic resonance: Theory and experiment," Proc. R. Soc. Lond. A **454**, 447-467 (1998).

[12] W. S. Warren, "The usefulness of NMR quantum computing," Science **277**, 1688-1689 (1997).

[13] N. Gershenfeld and I. L. Chuang, "Quantum computing with molecules," Sci. Am., June 1998, 50-55.

[14] N. Linden, H. Barjat, R. J. Carbajo, and R. Freeman, "Pulse sequences for NMR quantum computers: How to manipulate nuclear spins while freezing the motion of coupled neighbours," LANL e-print quant-ph/9811043.

[15] I. L. Chuang, L. M. K. Vandersypen, X. Zhou, D. W. Leung, and S. Lloyd, "Experimental realization of a quantum algorithm," Nature **393**, 143-146 (1998).

[16] J. A. Jones and M. Mosca, "Implementation of a quantum algorithm to solve Deutsch's problem on a nuclear magnetic resonance quantum computer," J. Chem. Phys. **109**, 1648-1653 (1998).

[17] N. Linden, H. Barjat, and R. Freeman, "An implementation of the Deutsch-Jozsa algorithm on a three-qubit NMR quantum computer," LANL e-print quant-ph/9808039.

[18] D. Collins, K. W. Kim, and W. C. Holton, "Deutsch-Jozsa algorithm as a test of quantum computation," Phys. Rev. A **58**, R1633-R1636 (1998).

[19] I. L. Chuang, N. Gershenfeld, and M. Kubinec, "Experimental implementation of fast quantum searching," Phys. Rev. Lett. **80**, 3408-3411 (1998).

[20] J. A. Jones, M. Mosca, and R. H. Hansen, "Implementation of a quantum search algorithm on a nuclear magnetic resonance quantum computer," Nature **393**, 344-346 (1998).

[21] D. G. Cory, M. D. Price, W. Maas, E. Knill, R. Laflamme, W. H. Zurek, T. F. Havel, and S. S. Somaroo, "Experimental quantum error correction," Phys. Rev. Lett. **81**, 2152-2155 (1998).

[22] D. Leung, L. Vandersypen, X. Zhou, M. Sherwood, C. Yannoni, M. Kubinec, and I. Chuang, "Experimental realization of a two bit phase damping quantum code," LANL e-print quant-ph/9811068.

[23] R. Laflamme, E. Knill, W. H. Zurek, P. Catasti, and S. V. S. Mariappan, "NMR Greenberger-Horne-Zeilinger states," Philos. Trans. R. Soc. Lond. A **356**, 1941-1948 (1998).

[24] S. Lloyd, "Microscopic analogs of the Greenberger-Horne-Zeilinger experiment," Phys. Rev. A **57**, R1473-R1476 (1998).

[25] M. A. Nielsen, E. Knill, and R. Laflamme, "Complete quantum teleportation using nuclear magnetic resonance," Nature **396**, 52-55 (1998).

[26] J. A. Jones and M. Mosca, "Approximate quantum counting on an NMR ensemble quantum computer," LANL e-print quant-ph/9808056.

[27] J. A. Jones, R. H. Hansen, and M. Mosca, "Quantum logic gates and nuclear magnetic resonance pulse sequences," LANL e-print quant-ph/9805070; J. Magn. Resonance **135**, 353-360 (1998).

[28] D. Deutsch and R. Jozsa, "Rapid solution of problems by quantum computation," Proc. R. Soc. Lond. A **439**, 553-558 (1992).

[29] R. R. Ernst, G. Bodenhausen, and A. Wokaun, *Principles of Nuclear Magnetic Resonance in One and Two Dimensions* (Clarendon Press, Oxford, 1991).